The role of deformation in the ^{17}C structure and its influence in transfer and breakup reactions

P. Punta[1,*], *J. A.* Lay[1,2,**], and *A. M.* Moro[1,2,***]

[1]Departamento de FAMN, Facultad de Física, Universidad de Sevilla, Apartado 1065, E-41080 Sevilla, Spain
[2]Instituto Interuniversitario Carlos I de Física Teórica y Computacional (iC1), Apdo. 1065, E-41080 Sevilla, Spain

Abstract. ^{17}C structure is studied within a two-body model, a weakly bound neutron moving in a deformed potential generated by the *core*. A semi-microscopic method has been used to generate the deformed valence-core potential. The method consists of the convolution of a realistic nucleon-nucleon (NN) interaction with the core transition densities, which are obtained by antisymetrized molecular dynamics (AMD). The results highlight the important role of deformation for this nucleus and can be easily applied to reaction calculations.

1 Introduction

The study of nuclei far from the stability line is one of the main topics in current nuclear physics research. Due to its excess of neutrons, ^{17}C is an example of these so-called exotic nuclei. It is a specially interesting case, because it is a weakly bound nucleus whose first exited sate is a strong candidate for halo nature.

In this contribution, we present a semimicroscopic model for ^{17}C nucleus, described as a neutron+*core* two-body system. The purpose is to have a model sufficiently manageable to be applied to calculations of transfer and breakup reactions but yet providing a realistic description of the ^{17}C low-lying spectrum. Weakly bound nuclei are conveniently described within few-body models, which usually ignore possible deformation of the fragments. However, *core deformations* are known to significantly affect both the structure and dynamics of these systems. For this reason, the structure of different weakly bound nuclei has been studied using deformed two-body models such as the particle-rotor or the particle-vibrator. For example, the particle-rotor model has been successfully applied to the study of the structure and resonant breakup of ^{11}Be [1–4]. In the present contribution, the application of a more sophisticated semi-microscopic model to the ^{17}C system is detailed.

2 Semi-microscopic particle-plus-AMD model

In the weak-coupling limit, the Hamiltonian of our two-body system can be written as

$$\mathcal{H} = T(\vec{r}) + h_{core}(\xi) + V_{vc}(\vec{r},\xi) + V_{\ell s}(r)(\vec{\ell}\cdot\vec{s}). \quad (1)$$

where $T(\vec{r})$ is the kinetic energy operator for the relative motion between the valence particle and the core, $h_{core}(\xi)$ is the Hamiltonian of the core and $V_{vc}(\vec{r},\xi)$ is the effective valence-core interaction. A phenomenological spin-obit term with the usual radial dependence $V_{\ell s}(r)$ is added to the effective interaction. The variable ξ denotes the internal coordinates of the core, so the dependence of $V_{vc}(\vec{r},\xi)$ on it accounts for core excitation effects.

The eigenfunctions of the Hamiltonian, for a given energy ε, can be characterized by the parity π and the total angular momentum $\vec{J}$, resulting from the coupling of the angular momentum $\vec{j}$ of the valence particle to the core angular momentum $\vec{I}$. These functions can be generically expressed as

$$\Psi^{J^\pi}_{\varepsilon M}(\vec{r},\xi) = \sum_\alpha R^{J^\pi}_{\varepsilon\alpha}(r)\left[\mathcal{Y}^j_{\ell s}(\hat{r})\otimes\phi_I(\xi)\right]_{JM}, \quad (2)$$

where $\vec{\ell}$ is the orbital angular momentum between the valence particle and core, which couples to the spin of the valence particle $\vec{s}$ to give the particle total angular momentum $\vec{j}$. The label α denotes the set of quantum numbers $\{\ell, s, j, I\}$.

In our semi-microscopic model, the $V_{vc}(\vec{r},\xi)$ interaction is calculated convoluting an effective inmedium NN interaction with microscopic transition densities of the core nucleus. In the present case, the NN interaction from Jeukenne, Lejeune, and Mahaux (JLM) is used [5]. The required transition densities are obtained from the antisymmetrized molecular dynamics (AMD) calculation [6, 7]. The formalism of this model, that we will call PAMD, is explained in detail in [8], where it is applied to ^{11}Be and ^{19}C.

2.1 Diagonalization in the THO basis

The Hamiltonian presented above is diagonalized in a pseudo-state basis. Therefore, the eigenfunctions of

*e-mail: ppunta@us.es
**e-mail: lay@us.es
***e-mail: moro@us.es

Eq. (2) can be expressed as a linear combination of the basis functions. In our case, the transformed harmonic oscillator basis (THO) is chosen. This basis applies a locale scale transformation (LST) to the harmonic oscillator wave functions,

$$R^{THO}_{n\ell}(r) = \frac{s}{r}\sqrt{\frac{ds}{dr}} R^{HO}_{n\ell}[s(r)]. \quad (3)$$

$R^{HO}_{n\ell}(s)$ is the radial part of the usual HO functions and we adopted a parametric form for the LST, $s(r)$, from Karataglidis *et al.* [9]

$$s(r) = \left[\frac{1}{\left(\frac{1}{r}\right)^m + \left(\frac{1}{\gamma\sqrt{r}}\right)^m}\right]^{\frac{1}{m}}. \quad (4)$$

This basis has been successfully applied to the discretization of the continuum of weakly bound nuclei to describe breakup and transfer direct reactions both for two-body and three-body systems [10, 11].

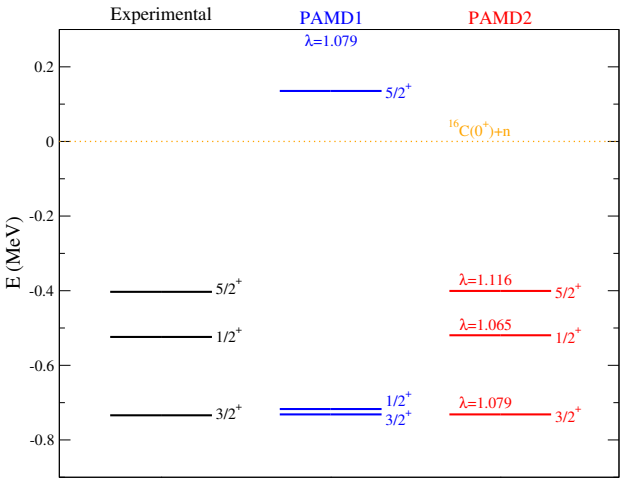

Figure 1. Experimental and calculated energy levels of ^{17}C. Starting from the left, the second column is the PAMD1 model, with a single renormalization factor, and the third the PAMD2, which uses different factors to reproduce the experimental values [14, 15].

3 Results of the application to ^{17}C

The method described above is applied to ^{17}C using the transition densities of ^{16}C from [7]. Some of the results of this model were first shown in [12] together with the discussion of the one-neutron transfer reaction ^{16}C(d,p). Here, a more detailed study of the ingredients of the model and its results is presented.

We assume that the only accessible core states are the ground state 0^+ and the first excited state 2^+. The latter is assigned the excitation energy of 1.766 MeV, which corresponds to the experimental energy of the first excited state of ^{16}C [13]. Furthermore, for the valence neutron, $\ell \leq 3$ is restricted.

In order to reproduce the experimental separation energy, $S_n = 0.734$ MeV [14], a global renormalization factor of $\lambda = 1.079$ needs to be applied to the effective potential $V_{vc}(\vec{r}, \xi)$. Although this factor is purely phenomenological, the change in interaction is less than 8%. This interaction is supplemented with a spin-orbit term with a standard strength of $V_{so} = 6$ MeV. It is parameterized, as usual, in terms of the derivative of a Wood-Saxon shape, and the values $R_{so} = 3$ fm, $a_{so} = 0.65$ fm are used to be consistent with the extension of the effective potential.

With these parameters, the Hamiltonian is diagonalized in the THO basis, giving rise to the energy levels shown in the central spectrum of figure 1. In the same figure, on the left, the experimental energies are shown [14, 15]. On the right are the renormalization λ factors that must be applied in each case to reproduce the experimental energies. Therefore, we distinguish between a PAMD1 model, which uses a single renormalization factor, and the PAMD2 model, which applies different factors according to the angular momentum of the ^{17}C state. The biggest difference with the PAMD1 model is that it obtains the second excited state $5/2^+_1$ as a resonance instead of a bound state. However, this resonance is located very close to the ^{17}C + n threshold, approximately 0.1 MeV above, with a difference of 0.5 MeV with respect to the experimental value. Similarly, the first excited state $1/2^+_1$ is only 0.2 MeV below the experimental level.

The functions $u_\alpha(r) = rR^{J^\pi}_{\varepsilon\alpha}(r)$, which describe the radial part of the wave function, are shown both for the ground state (figure 2) and for the two first excited states (figure 3). The ground state is the same for the PAMD1 and PAMD2 models, therefore its wave function is also identical. In the case of excited states, figure 3 compares the functions obtained for the PAMD1 and PAMD2 models. In the upper panel, they are compared for the first excited state $1/2^+_1$, and in the lower panel for the second excited state $5/2^+_1$. It can be verified that, in both cases, the wave functions are almost identical despite the energy differences of the states. For the $1/2^+_1$ case, our results support the halo nature of this state in view of the greater spatial extension of its associated wave function. This is quantitatively corroborated in table 1, where the mean square radii obtained for each state and model are shown. The values obtained for the first excited state are clearly larger than those obtained for the rest. As this state is less bound in the PAMD2 model, there is an appreciable increase in the mean square radius in this case. Note that, since the $5/2^+_1$ state appears as a resonance in the PAMD1 model, its root mean square radius is meaningless. In fact, in the lower panel of figure 3, it can be seen that the component $|d_{5/2} \otimes 0^+\rangle$ of this state does not vanish completely asymptotically for the PAMD1 model. Table 1 also shows the weights of the α components of the wave function for each state and each model. The differences between the values of the two models are not significant.

4 Conclusions and perspectives

Analyzing the results, the PAMD2 model does not have many advantages compared to PAMD1 model, aside from

Table 1. Weights of the components of the wave function and mean square radii for ^{17}C. The results obtained with the PAMD1 and PAMD2 models for the ground state and the two first excited states are shown

State	$3/2^+_{gs}$	$1/2^+_1$		$5/2^+_1$	
Model	PAMD1 - PAMD2	PAMD1	PAMD2	PAMD1	PAMD2
$\|(\ell s)j \otimes 0^+\rangle$	0.028	0.512	0.530	0.326	0.333
$\|s_{1/2} \otimes 2^+\rangle$	0.349	-	-	0.668	0.657
$\|d_{3/2} \otimes 2^+\rangle$	0.131	0.040	0.032	0.000	0.000
$\|d_{5/2} \otimes 2^+\rangle$	0.492	0.448	0.438	0.006	0.009
r_{ms} (fm)	4.030	5.246	5.748	-	4.480

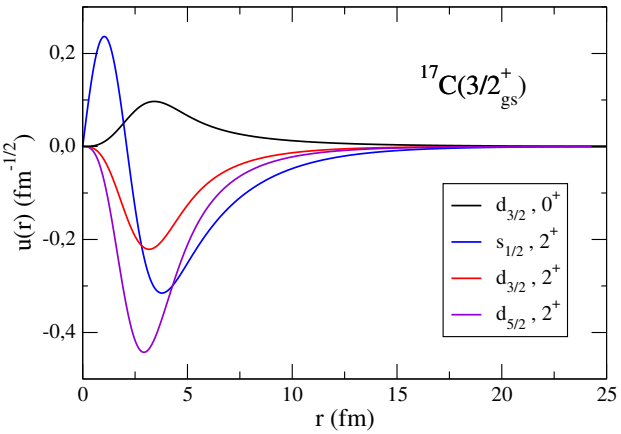

Figure 2. Radial part of the wave function obtained for the ground state of ^{17}C.

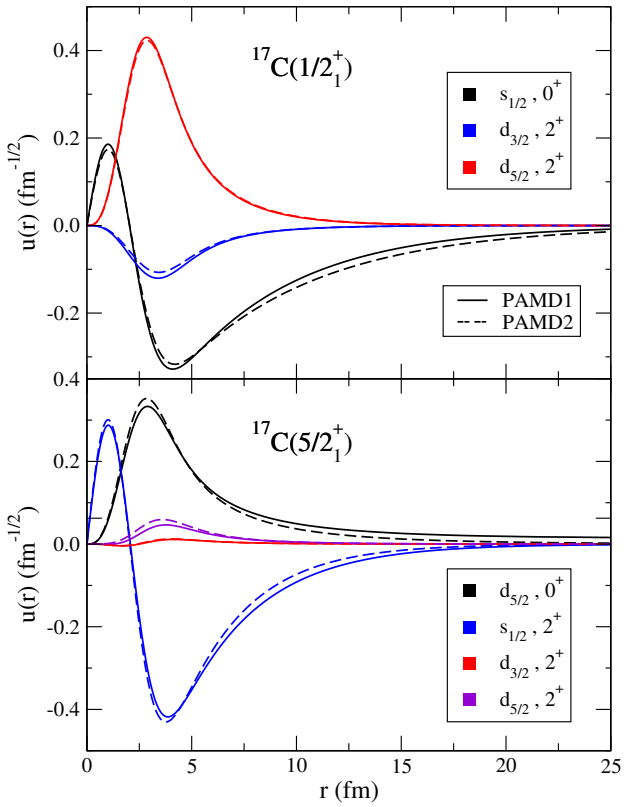

Figure 3. Radial part of the wave function obtained for the first excited state (upper panel) and second excited state of ^{17}C (lower panel). The results of the PAMD1 and PAMD2 models are compared

providing a better description of the energies. The inclusion of more phenomenological parameters in order to better reproduce the experimental energies of the bound states, does not cause significant changes in the wave functions of these states. Regarding the wave functions, there is a strong mixing of the components due to deformation, as shown by the weights in table 1. This is expected to produce strong effects on any reaction that depends on the structure of ^{17}C. These effects have already been proven for the case of ^{19}C, reaction calculations have been performed describing the ^{19}C structure with the same PAMD formalism [16].

Being a weakly bound nucleus, the study of one-neutron transfer reactions involving ^{17}C is especially interesting. Calculations for the reaction ^{16}C$(d,p)^{17}$C, for which there are recent experimental data from GANIL [12], are underway and the results will be presented soon. The referred work shows data of the angular distribution of the cross section for the transfer to the bound states of ^{17}C. The idea is that, to calculate this cross section theoretically, the overlap function $\langle^{17}\text{C}|^{16}\text{C}\rangle$ is required, which can be directly related to the functions $R^{J^\pi}_{\varepsilon\alpha}(r)$ obtained with the PAMD model.

In Ref. [12], spectroscopic factors (SF) for the $\langle^{17}\text{C}|^{16}\text{C}\rangle$ overlap were inferred from the comparison of the measured transfer data with ADWA calculations. In our assumed simplified two-body model, in which antisymmetrization between the valence neutron and the core is neglected, SF cannot be strictly obtained. However, as long as these antisymmetrization effects are not large, the weights listed in table 1 can be approximately regarded as SF and compared with the values from Ref. [12]. Therefore, as we start from ^{16}C in its ground state 0^+, the spectroscopic factors shown in [12] can be compared with the weights of the components $|(\ell s)j \otimes 0^+\rangle$ obtained with our model. For the $|d_{3/2} \otimes 0^+\rangle$ component of the ground state, a 0.3 factor is presented, perfectly compatible with our model. In the case of the $1/2^+_1$ state ($|s_{1/2} \otimes 0^+\rangle$), the range of values is between 0.5 and 1.0, so the values shown in table 1 fall in the lower part of the range. Nevertheless, the values we obtain for the component $|d_{5/2} \otimes 0^+\rangle$ of the $5/2^+_1$ state is below the experimental values ($0.5-0.7$), what can be a limitation of our structure model.

The study of the low-lying continuum of ^{17}C is also in progress, with the goal of extending the application

of the PAMD model to the transfer to the continuum for ^{16}C$(d, p)^{17}$C reaction. Furthermore, this model will be applied to the breakup reaction $^{17}\mathrm{C} + p \rightarrow^{16} \mathrm{C} + n + p$, for which there are already published data [17].

Acknowledgments

The present research is funded from grant PID2020-114687GB-I00 by MCIN/AEI/10.13039/501100011033, the project PAIDI 2020 with Ref. P20_01247 by the Consejería de Economía, Conocimiento, Empresas y Universidad, Junta de Andalucía (Spain), and by ERDF A way of making Europe. P.P. acknowledges PhD grants from the Ministerio de Universidades and the Consejería de Transformación Económica, Industria, Conocimiento y Universidades, Junta de Andalucía

References

[1] J.A. Lay, A.M. Moro, J.M. Arias, J. Gómez-Camacho, Phys. Rev. C **85**, 054618 (2012)
[2] A.M. Moro, J.A. Lay, Phys. Rev. Lett. **109**, 232502 (2012)
[3] V. Pesudo, M.J.G. Borge, A.M. Moro, J.A. Lay, E. Nácher, J. Gómez-Camacho, O. Tengblad, L. Acosta, M. Alcorta, M.A.G. Alvarez et al., Phys. Rev. Lett. **118**, 152502 (2017)
[4] A.M. Moro, J.A. Lay, J. Gómez Camacho, Physics Letters B **811**, 135959 (2020)
[5] J.P. Jeukenne, A. Lejeune, C. Mahaux, Phys. Rev. C **16**, 80 (1977)
[6] Y. Kanada-En'yo, H. Horiuchi, A. Ono, Phys. Rev. C **52**, 628 (1995)
[7] Y. Kanada-En'yo, F. Kobayashi, T. Suhara, Journal of Physics: Conference Series **445**, 012037 (2013)
[8] J.A. Lay, A.M. Moro, J.M. Arias, Y. Kanada-En'yo, Phys. Rev. C **89**, 014333 (2014)
[9] S. Karataglidis, K. Amos, B.G. Giraud, Phys. Rev. C **71**, 064601 (2005)
[10] J.A. Lay, A.M. Moro, J.M. Arias, J. Gómez-Camacho, Phys. Rev. C **82**, 024605 (2010)
[11] J. Casal, E. Garrido, R. de Diego, J.M. Arias, M. Rodríguez-Gallardo, Phys. Rev. C **94**, 054622 (2016)
[12] X. Pereira-López et al., Phys. Lett. B **811**, 135939 (2020)
[13] D. Tilley, H. Weller, C. Cheves, Nuclear Physics A **564**, 1 (1993)
[14] W. Meng, G. Audi, F.G. Kondev, S. Naimi, Chinese Physics C **41**, 030003 (2017)
[15] Z. Elekes et al., Phys. Lett. B **614**, 174 (2005)
[16] J.A. Lay, R. de Diego, R. Crespo, A.M. Moro, J.M. Arias, R.C. Johnson, Phys. Rev. C **94**, 021602 (2016)
[17] Y. Satou et al., Phys. Lett. B **660**, 320 (2008)